Semidark Higgs boson decays: Sweeping the Higgs neutrino floor

J. A. Aguilar-Saavedra,[1,*] J. M. Cano,[1,2,†] D. G. Cerdeño,[1,2,‡] and J. M. No[1,2,§]

[1]*Instituto de Fisica Teorica, IFT-UAM/CSIC, Cantoblanco, 28049 Madrid, Spain*

[2]*Departamento de Fisica Teorica, Universidad Autonoma de Madrid, Cantoblanco, 28049 Madrid, Spain*

(Received 20 June 2022; accepted 26 November 2022; published 21 December 2022)

We study exotic Higgs decays $h \to ZX$, with X an invisible beyond the Standard Model (SM) particle, resulting in a semidark final state. Such exotic Higgs decays may occur in theories of axionlike particles (ALPs), dark photons or pseudoscalar mediators between the SM and dark matter. The SM process $h \to Z\nu\bar{\nu}$ represents an irreducible "neutrino floor" background to these new physics searches, providing also a target experimental sensitivity for them. We analyze $h \to Z +$ invisible searches at the LHC and a future ILC, showing that these exotic Higgs decays can yield sensitivity to unexplored regions of parameter space for ALPs and dark matter models.

DOI: 10.1103/PhysRevD.106.115023

I. INTRODUCTION

The Higgs boson discovered at the Large Hadron Collider (LHC) offers a unique window into new physics, and it is paramount to study its properties with precision. Exotic Higgs decays, i.e., decays of the Higgs boson not present in the Standard Model (SM), constitute a primary avenue to probe the existence of new physics [1]. In the last years, there has been an intense experimental program at the LHC to search for such exotic Higgs decays [2–13] (see also [14] and references therein). Such searches have mainly targeted either fully visible final states, e.g., $h \to 2f2f'$ (with f, f' SM fermions) or a fully invisible Higgs decay (so-called invisible Higgs width).

Considering all/part of the Higgs boson decay products in these exotic decays to be invisible at colliders is well-motivated theoretically, e.g., if the Higgs boson directly interacts with a dark (i.e., not feeling the SM gauge interactions) sector of Nature, possibly containing the dark matter (DM) particle(s), or if the Higgs decay products are very long-lived and decay outside the LHC detectors.

Yet, partially invisible (semidark) Higgs boson decays constitute a much less explored avenue to search for new physics beyond the SM (BSM) coupled to the Higgs boson, and studies of these semidark Higgs decays exist in the literature for very few BSM scenarios [15,16] (see [17–21] for existing experimental searches). Such searches are fully complementary to searches for invisible Higgs decays, and generally probe different regions of parameter space of the same BSM theories. Semidark Higgs decays allow in particular to obtain key information on the nature of the coupling between the Higgs and the invisible state(s), by reconstructing the visible part of the exotic Higgs decay.

In this work we target the previously unexplored semidark Higgs decay $h \to ZX$, with X a BSM particle invisible at the LHC (manifesting as missing transverse energy $\not{E}_T$), and we show it is a promising avenue to probe various well-motivated BSM scenarios: X could be an axionlike particle (ALP) or dark photon that decays invisibly or is long-lived, escaping the detector. It could also be a pseudoscalar mediator particle between the SM and a dark sector of Nature containing the DM particle.[1]

We focus our study on the leptonic decay of the Z boson, $Z \to \ell\ell$ (with $\ell = e, \mu$), leading to the Higgs final state $h \to ZX \to \ell\ell + \not{E}_T$. Incidentally, the SM decays $h \to ZZ^* \to \ell\ell\nu\bar{\nu}$ and $h \to WW^* \to \ell\nu\ell\bar{\nu}$ yield the same final state. For the latter, the two leptons do not reconstruct the Z boson mass $m_Z \simeq 91$ GeV in general, which can be used to tell apart $h \to ZX$ from this SM decay process. However, $h \to ZZ^* \to \ell\ell\nu\bar{\nu}$ completely mimics a possible BSM signal. The SM decay $h \to Z\nu\bar{\nu}$ then constitutes a "neutrino floor"[2] to experimental searches for new physics in the

*ja.a.s@csic.es
†josem.cano@uam.es
‡davidg.cerdeno@gmail.com
§josemiguel.no@uam.es

[1]A pseudoscalar mediator would nicely explain the absence of a spin-independent signal in current DM direct detection experiments [22]. These pseudoscalar portal to DM scenarios have also been proposed to explain [23–25] the γ-ray excess [26,27] in the Fermi-LAT observations of the Milky Way Galactic Center [28].

[2]In analogy to DM direct detection experiments, where coherent elastic neutrino-nucleus scattering can pose an irreducible background to DM searches, known as the "neutrino floor" [29].

semidark $h \to ZX$ ($X \to \not{E}_T$) channel, below which a possible BSM signal would be buried. It also provides a target sensitivity for the $h \to ZX$ ($X \to \not{E}_T$) search at the LHC and future colliders which would guarantee a detection (albeit in that case not of BSM physics), given by the SM branching fraction $\mathrm{BR}(h \to Z\nu\bar{\nu})_{\mathrm{SM}} = 5.4 \times 10^{-3}$ [30].

The rest of the paper is organized as follows: In Sec. II we motivate the specific LHC Higgs production mode chosen for our study and analyze (in a model-independent fashion) the sensitivity of LHC searches for semidark Higgs decays $h \to Z + \not{E}_T$. In Sec. III we perform a similar study for the future e^+e^- International Linear Collider (ILC). Then, in Sec. IV we showcase the power of our proposed search for several concrete BSM scenarios.

II. LHC SEARCHES FOR $h \to ZX \to \ell\ell + \not{E}_T$

We consider for the rest of this work an LHC center-of-mass energy $\sqrt{s} = 14$ TeV, and do not make for the time being any reference to the specific nature of X beyond it being invisible at colliders. As a first step in our analysis, we discuss the feasibility to search for the $h \to ZX \to \ell\ell + \not{E}_T$ exotic Higgs decay using the different Higgs boson production modes at the LHC. Our analysis reveals the convenience of focusing on the production of the Higgs boson at the LHC in association with a Z boson, $pp \to Zh$: For gluon-fusion (ggF) and vector boson fusion (VBF) Higgs production channels, the Higgs is either produced on its own (ggF) or recoiling against jets (ggF, VBF). Since the phase space for the Higgs decay $h \to ZX$ is fairly small (as $(m_h - m_Z)/m_h \ll 1$), an accurate $\not{E}_T$ reconstruction may be limited by the transverse momentum (p_T) resolution of the jets. In addition, the $\ell\ell + \not{E}_T +$ jets final state has very large SM backgrounds, in particular reducible ones if the $\not{E}_T$ reconstruction is not perfect. Higgs production in association with an electroweak gauge boson, $pp \to W^{\pm}h$ and $pp \to Zh$, is thus better suited for the $h \to ZX$ ($X \to \not{E}_T$) exotic Higgs decay search at the LHC. Yet, the leptonic decay of the W boson in $pp \to Wh$ adds $\not{E}_T$ to the final state, making it challenging to disentangle this contribution from the Higgs boson decay products. In addition, the LHC cross section for the dominant SM background in this case, $pp \to W^{\pm}Z$, is very large, $\mathcal{O}(50)$ pb. In contrast, for $pp \to Zh$ ($h \to Z + \not{E}_T$) the leptonic decay of both Z bosons offers a sharp reconstruction of the two dilepton resonances together with an accurate $\not{E}_T$ measurement, combined with SM backgrounds that can be efficiently suppressed or are very small to begin with, as we discuss in detail below.

For our analysis, we generate the BSM signal specifically using a FeynRules [31] implementation of the two-Higgs-doublet model plus pseudoscalar singlet (2HDM + a) extension of the SM (see e.g., [32–34]), through the decay $h \to Za$ (with a invisible). Our results apply to any two-body Higgs decay $h \to ZX$, $X \to \not{E}_T$. Both Z bosons from the signal are considered to decay leptonically, $Z \to \ell\ell$. The relevant SM backgrounds are $pp \to ZZ \to 4\ell$ (with $\not{E}_T$ appearing via mis-measurements and detector effects), $pp \to ZZZ, WWZ \to 4\ell + 2\nu$, $pp \to t\bar{t}Z, tWZ \to 4\ell + 2\nu +$ jets, and $pp \to Zh$ ($h \to WW^* \to 2\ell + 2\nu$). We generate signal and SM background event samples with MG5_AMC@NLO [35] (using the NNPDF31_NNLO [36] parton distribution functions) with subsequent parton showering and hadronization via PYTHIA 8 [37] and detector simulation via DELPHES [38], using the detector card designed for High Luminosity (HL)-LHC studies. We normalize the respective cross sections to their next-to-leading-order (NLO) in QCD values, obtained from the literature [39,40] (for the $pp \to Zh$ and $pp \to ZZ$ processes the normalization is however performed to the NNLO cross section [30,41]; to avoid known issues at NLO in QCD related to real b-quark emission [42,43], tWZ is kept at LO with a negligible impact on our analysis). Selected events are required to contain exactly four reconstructed leptons after detector simulation, comprising two pairs of opposite-sign, same-flavor leptons. Events must pass the single, two or three-lepton trigger requirements from the ATLAS 2018 Trigger menu [44]. When multiple dilepton combinations satisfying the selection requirements exist, the one minimizing $\Delta^2 = m_Z^{-2}[(m_{\ell\ell_1} - m_Z)^2 + (m_{\ell\ell_2} - m_Z)^2]$ (with $m_{\ell\ell_i}$ the dilepton invariant masses) is chosen. Extra hadronic activity is vetoed by rejecting events with either b-tagged jets or hard jets with $p_T > 50$ GeV.

Since the Higgs decay is partially invisible, its invariant mass cannot be fully reconstructed, nor can the dilepton pair from its decay be straightforwardly identified. The latter is key to better exploit the kinematic properties of the BSM signal in the analysis. We may identify the dilepton pair corresponding to the Z boson from the Higgs decay using the transverse mass M_T, given by $M_T^2 = \left(\sqrt{m_{\ell\ell}^2 + |\vec{p}_T^{\,\ell\ell}|^2} + \not{E}_T\right)^2 - |\vec{p}_T^{\,\ell\ell} + \vec{\not{E}}_T|^2$, with $\vec{\not{E}}_T$ and $\vec{p}_T^{\,\ell\ell}$ the missing transverse 3-momentum and Z boson transverse 3-momentum, respectively; a complementary approach would be to select the Z boson closest to $\vec{\not{E}}_T$ in the azimuthal plane as the one from the Higgs decay. Figure 1 shows the M_T (top) and $\Delta\phi(Z, \vec{\not{E}}_T)$ (azimuthal angle between $\vec{\not{E}}_T$ and the 3-momentum of the dilepton pair, bottom) distributions for the leptonically decaying Z boson from the Higgs decay (labeled as Z_1) and the Z boson produced in association with the Higgs (labeled as Z_2). To optimally exploit the event kinematic information in identifying Z_1 and Z_2 for the BSM signal, we build a neural network (NN) (two hidden layers, 32 nodes each, using rectified linear unit activation for the hidden layers and a sigmoid function for the output) which takes as input M_T and $\Delta\phi(Z, \vec{\not{E}}_T)$ for both dilepton pairs.

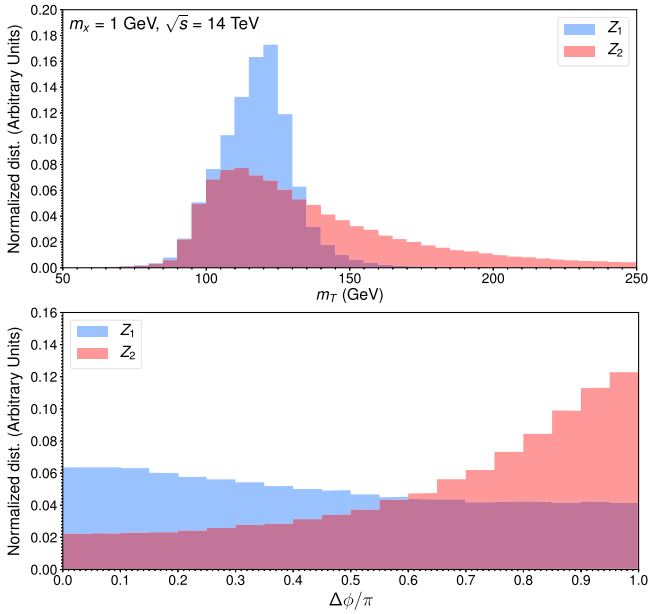

FIG. 1. M_T (top) and $\Delta\phi(Z, \vec{\not{E}}_T)/\pi$ (bottom) for Z_1 (blue) and Z_2 (red), see text for details.

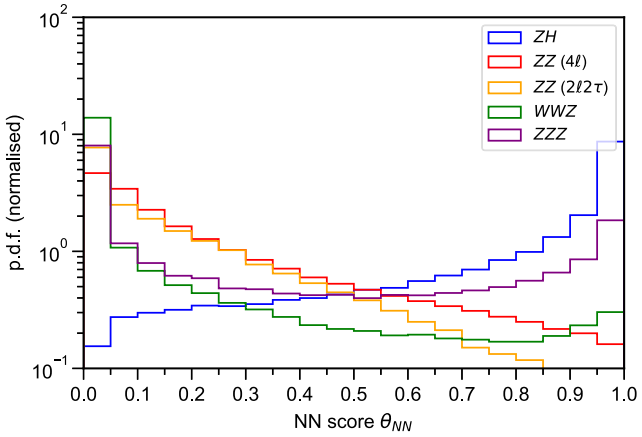

FIG. 2. Score θ_{NN} of the neural network discriminating BSM signal vs SM background in our analysis, for the BSM signal with $m_X = 1$ GeV (labeled ZH, blue), and the relevant SM backgrounds: $ZZ \to 4\ell$ (red), $ZZ \to 2\ell 2\tau$ (yellow), $WWZ \to 4\ell + 2\nu$ (green), $ZZZ \to 4\ell + 2\nu$ (purple).

The correct and wrong Z_i assignments for the NN training are labeled using generator-level information. The NN is trained with a Monte Carlo sample of 20,000 signal events (not used in our subsequent analysis) with $m_X = 1$ GeV, using the Adam algorithm for the optimization. The efficiency obtained for a correct $Z_{1,2}$ choice for the signal is 73%, and the NN is then applied in our sensitivity analysis to both the BSM signal (for $m_X \in [1, 32.5]$ GeV) and the SM backgrounds.

The signal cross section (for $\mathrm{BR}(h \to ZX) = 1$, $\mathrm{BR}(X \to \not{E}_T) = 1$ and $m_X = 1$ GeV) after the initial event selection is 1.420 fb. The respective SM background cross sections after event selection are 25.6 fb for $ZZ \to 4\ell$, 0.76 fb for $ZZ \to 2\ell + 2\tau$, 0.169 fb for $WW^{(*)}Z \to 4\ell + 2\nu$ (including the $pp \to Zh$, $h \to WW^*$ contribution), 0.012 fb for $ZZZ \to 4\ell + 2\nu$, and 0.044 fb for $t\bar{t}Z, tWZ \to 4\ell + 2\nu +$ jets. Our $h \to ZX$ LHC signal region must target relatively high-p_T Zh associated production, with reconstructed Z-boson resonances for the two dilepton pairs and the Higgs transverse mass M_T from the Z_1 dilepton candidate. Requiring a moderately large amount of $\not{E}_T$, demanding Z_1 to be well-aligned with $\vec{\not{E}}_T$ in the azimuthal plane and rejecting events with a large rapidity gap between dilepton pairs also improves the sensitivity of the analysis.

The rich event kinematics (four visible objects in the final state plus the missing transverse energy) indicates that a multivariate approach which accesses the full kinematic information of the events could enhance our BSM signal sensitivity. We use another NN (two hidden layers of 256 nodes, same activation functions and optimization as before) for the discrimination between signal and SM background, with input variables: $\not{E}_T$, $m_{4\ell}$ (four-lepton invariant mass), $m_{\ell\ell_1}$ and $m_{\ell\ell_2}$, $\Delta\phi(Z_1, \vec{\not{E}}_T)$ and $\Delta\phi(Z_2, \vec{\not{E}}_T)$, M_T (built from Z_1), $p_T^{\ell\ell_1}$ and $p_T^{\ell\ell_2}$ (dilepton transverse momenta), $p_T^{\ell_1}$, $p_T^{\ell_2}$, $p_T^{\ell_3}$, $p_T^{\ell_4}$ (transverse momenta of the four leptons, ordered from higher to lower) and $(p_T^{\ell\ell_2} + \not{E}_T)/p_T^{\ell\ell_1}$. The NN is trained with an unbalanced Monte Carlo set dominated by $ZZ \to 4\ell$ events, precisely to optimize the rejection of this SM background (as it has by far the largest LHC cross section among SM backgrounds). The NN score θ_{NN} for the $m_X = 1$ GeV signal and relevant SM backgrounds is shown in Fig. 2 (for X of spin-1, angular correlations in the Z_1 dilepton pair mildly differ from the spin-0 X case, yet our signal sensitivity results would be nearly unchanged).

Our signal region is defined for HL-LHC as $\theta_{NN} \geq 0.997$. The resulting signal and SM background efficiencies (evaluated on the NN test sets) are 0.12, 1.5×10^{-4}, 2.8×10^{-5}, 0.0013, 0.012, 0.0016, and $< 9.4 \times 10^{-4}$, respectively for the signal (with $m_X = 1$ GeV), $ZZ \to 4\ell$, WWZ, $ZZ \to 2\ell + 2\tau$, ZZZ, tWZ, and $t\bar{t}Z$. We employ the "Asimov estimate" [45] (since $\mathcal{O}(s/b)$ is not small) to derive the 2σ exclusion sensitivity on $\mathrm{BR}(h \to ZX) \times \mathrm{BR}(X \to \not{E}_T)$ with the 3 ab^{-1} of integrated luminosity from HL-LHC, in the range $m_X \in [1, 32.5]$ GeV (our results may also be directly extrapolated to the $m_X \to 0$ limit). We find our NN results to improve by ~30% the sensitivity of a cut-and-count analysis, and come close to probing the Higgs neutrino floor (for $m_X = 1$ GeV, it probes $\mathrm{BR}(h \to ZX) \times \mathrm{BR}(X \to \not{E}_T) = 2.8 \times \mathrm{BR}(h \to Z\nu\bar{\nu})_{\mathrm{SM}}$ at 2σ).

We repeat our analysis for an integrated luminosity of 300 fb^{-1}, with a less stringent signal region cut $\theta_{NN} \geq 0.985$ to increase the fraction of signal events surviving the selection. The sensitivity results for 300 fb^{-1} and 3 ab^{-1} (HL-LHC) are shown in Fig. 3.

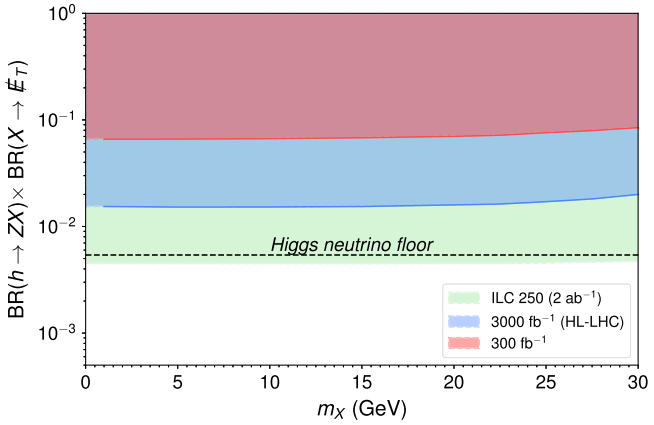

FIG. 3. 2σ exclusion sensitivity for $\mathrm{BR}(h \to ZX) \times \mathrm{BR}(X \to \not{E}_T)$ as a function of m_X for an LHC integrated luminosity of 300 fb^{-1} (red) and 3000 fb^{-1} (HL-LHC, blue). The Higgs neutrino floor is shown as a dashed-black line. The ILC $\sqrt{s} = 250$ GeV (2 ab^{-1}) would-be sensitivity is shown in green.

III. ILC SEARCHES FOR $h \to ZX \to \ell\ell + \not{E}_T$

A future International Linear Collider [46,47] operating at $\sqrt{s} = 250$ GeV would be able to probe $\mathrm{BR}(h \to ZX)$ down to the *Higgs neutrino floor* by exploiting several advantages over the LHC search discussed in the previous section: (i) Higgstrahlung $e^+e^- \to Zh$ is now the dominant Higgs production mode; (ii) The e^+e^- collisions at ILC offer a much cleaner environment (largely void of hadronic activity) and the 3-momenta of the incoming particles is known up to radiative and smearing effects, allowing for full missing momentum reconstruction; (iii) The Higgs recoil mass, constructed from the Z-boson recoiling against the Higgs boson (Z_2) as $M^2_{\mathrm{reco}} = s + m^2_{Z_2} - 2E_{Z_2}\sqrt{s}$, provides a straightforward way to correctly identify $Z_{1,2}$ for the BSM signal (M_{reco} built out of the Z-boson from the Higgs decay, Z_1, will not present any resonant structure).

For our analysis, we specifically consider $\sqrt{s} = 250$ GeV with 2 ab^{-1} of integrated luminosity (90% of it evenly split between the two opposite beam helicities) and beam polarizations being 80% for the electrons and 30% for the positrons respectively [47]. Again, we consider the SM Higgs produced in association with a Z-boson, $e^+e^- \to Zh$ for our BSM signal. The relevant SM backgrounds are now $e^+e^- \to ZZ$ ($\to 4\ell, 2\ell + 2\tau$), $e^+e^- \to WWZ$ and $e^+e^- \to ZZ\nu\bar{\nu}$ (including VBF initiated contributions; Higgs mediated contributions correspond to the SM Higgs neutrino floor, and are not included) Our signal and background event generation is performed as in the previous section, using in this case the DELPHES detector card designed for ILC studies [38,48] (a study of lepton collider capabilities including the effects of initial state radiation or beamstrahlung is left for future work).

Our initial event selection mimics that of the previous LHC analysis. The cross sections for the signal (for $\mathrm{BR}(h \to ZX) = 1$ and $m_X = 1$ GeV) and SM backgrounds after event selection are respectively 1.421 fb, 5.64 fb (for $ZZ \to 4\ell$), 0.13 fb (for $ZZ \to 2\ell 2\tau$), 0.073 fb (for $WW^{(*)}Z \to 4\ell + 2\nu$, dominated by the $e^-e^+ \to Zh$, $h \to WW^*$ contribution), and 0.011 ab (for $ZZ\nu\bar{\nu} \to 4\ell + 2\nu$). For the ILC environment, the use of a NN does not offer such a strong advantage over a simpler (cut-and-count) analysis. We thus define our kinematic region for signal extraction in the latter way: we demand reconstructed Z-boson resonances for the two dilepton pairs, $m_{Z_1} \in [55, 100]$ GeV, $m_{Z_2} \in [80, 105]$ GeV; we require the recoil mass constructed out of Z_2 in the range $M_{\mathrm{reco}} \in [120, 135]$ GeV, together with $p_{Z_2} > 50$ GeV and $\not{E} \in [5, 60]$ GeV (p_{Z_2}, $\not{E}$ respectively the modulus of the Z_2 dilepton candidate's 3-momentum and the modulus of the missing 3-momentum); the invariant mass $m^{\mathrm{miss}}_{Z_1}$ built from Z_1 and $\vec{\not{E}}$, given by $(m^{\mathrm{miss}}_{Z_1})^2 = \left(\sqrt{m^2_{Z_1} + p^2_{Z_1}} + \not{E}\right)^2 - |\vec{p}_{Z_1} + \vec{\not{E}}|^2$, is required to reconstruct the 125 GeV Higgs mass, $m^{\mathrm{miss}}_{Z_1} \in [95, 130]$ GeV; we further require $m_{4\ell} > 160$ GeV, $(p_{Z_1} + \not{E})/p_{Z_2} < 1.8$ and $(m^{\mathrm{miss}}_{Z_2})^2 = \left(\sqrt{m^2_{Z_2} + p^2_{Z_2}} + \not{E}\right)^2 - |\vec{p}_{Z_2} + \vec{\not{E}}|^2 > (95\,\mathrm{GeV})^2$. These signal region cuts have an efficiency of 0.89 for the BSM signal (for $m_X = 1$ GeV), and 1.7×10^{-5}, 0.013, 0.085, 0.24 for the $ZZ \to 4\ell$, $ZZ \to 2\ell 2\tau$, WWZ, and $ZZ\nu\bar{\nu}$ SM backgrounds, respectively. Using the "Asimov estimate", we derive a 2σ sensitivity $\mathrm{BR}(h \to ZX) \times \mathrm{BR}(X \to \not{E}) = 0.0045$. We show the corresponding ILC sensitivity as a function of m_X in Fig. 3. We note that this sensitivity lies below the SM Higgs neutrino floor, not been included in our analysis. This means that we should now instead consider the ILC discovery potential of $\mathrm{BR}(h \to Z\nu\bar{\nu})_{\mathrm{SM}}$; the expected significance over the background only hypothesis reaches 2.4σ (the significance may be enhanced to $\sim 4\sigma$, at the expense of our BSM analysis not yielding a uniform sensitivity in m_X). ILC can thus sweep the entire new physics parameter space of semidark Higgs decays down to the Higgs neutrino floor.

IV. CONSTRAINTS ON SPECIFIC MODELS

A. Axionlike particles

The existence of interactions between the SM Higgs and light axionlike particles is a well-motivated BSM possibility [49,50]. Exotic Higgs decays represent a key experimental signature in this case. The Higgs boson partial decay width into a SM Z-boson and the ALP a is $\Gamma(h \to Za) = (m_h^3/16\pi f_a^2) c^2_{aZh} \lambda^{3/2}$, with f_a the ALP decay constant, $\lambda = (1 - (m_Z^2 - m_a^2)/m_h^2)^2 - 4m_Z^2 m_a^2/m_h^4$ and c_{aZh} the Wilson coefficient for the effective operator that couples the ALP to the SM Higgs field (which we leave here unspecified, see [49,50] for details). If a then couples to some hidden sector particle(s) (see e.g., [51,52]), its

dominant decay mode(s) may be into the dark sector, thus invisible at colliders. This encompasses the intriguing possibility that the ALP may be a mediator between the SM and the DM candidate [51]. Higgs decays $h \to Za$, $a \to \not{E}_T$ can then probe such ALP scenarios.

To translate the model-independent LHC and ILC projected sensitivities from the previous sections into a probe of the parameter space of ALPs, we specifically consider, together with the coupling between the ALP and the SM Higgs, an ALP coupling to a hidden fermion χ, given by $y_\chi \bar{\chi}\gamma^\mu\gamma^5\chi\partial_\mu a/f_a$ as well as an ALP coupling to photons $c_{a\gamma\gamma}/f_a a F^{\mu\nu}\tilde{F}_{\mu\nu}$ (we do not include an ALP coupling to gluons or SM fermions for simplicity). y_χ does not have a preferred value, while the expectation for the bosonic Wilson coefficient is $c_{a\gamma\gamma} \sim \alpha_{\rm EM}$ (the electromagnetic coupling constant) [53]. We then set $c_{a\gamma\gamma} = \alpha_{\rm EM}(Q)$ (Q being the energy scale of the process considered), and $y_\chi = 1$, $c_{aZh} = 1$, $m_\chi = 0.45 m_a$ (to allow for the invisible ALP decay $a \to \chi\bar{\chi}$), and show in Fig. 4 the LHC projected 2σ sensitivity on $\mathrm{BR}(h \to Za) \times \mathrm{BR}(a \to \chi\bar{\chi})$ in the (m_a, f_a) plane. We also depict the Higgs neutrino floor, within reach of the $\sqrt{s} = 250$ GeV ILC. Figure 4 also shows, under the assumption that χ is the DM particle, the $(m_a,\ f_a)$ relation yielding (for the choice of parameters described above) the observed DM relic abundance $\Omega_{\rm DM}h^2 = 0.12$ [54] generated via thermal freeze-out in the early Universe (taken from [51]), as well as the existing and projected constraints on this ALP scenario from searches at LEP, LHC and flavor factories (*BABAR*, Belle-II), and astrophysics (supernova 1987A), all detailed in Appendix A. Finally, we also show in Appendix A the corresponding limits on the (m_a, f_a) plane if a hypercharge coupling $c_{aBB}/f_a a B^{\mu\nu}\tilde{B}_{\mu\nu}$ (rather than a coupling only to photons) is assumed for the ALP.

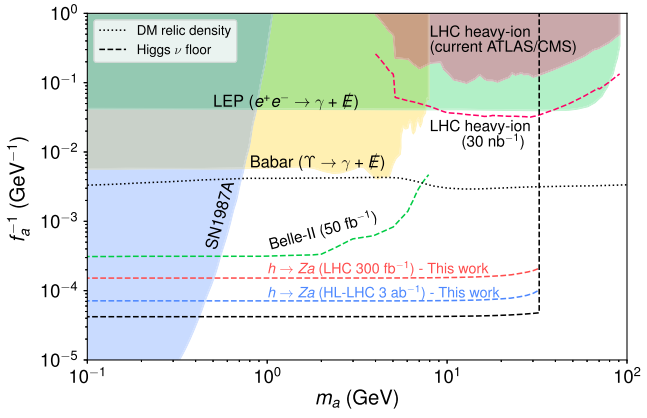

FIG. 4. Present (solid) and projected (dashed) constraints on the $(m_a,\ f_a)$ plane for an ALP with coupling to photons, a hidden (DM) fermion χ and the SM Higgs (via a c_{aZh} coupling), see text for details.

B. Pseudoscalar portal to dark matter

Two Higgs doublet models (2HDM) extended by a singlet pseudoscalar mediator (2HDM + a) and a fermionic singlet DM particle constitute the minimal renormalizable realization of a pseudoscalar portal to DM [25,32–34,55], which avoids the stringent existing DM direct detection constraints [22] (it yields a spin-independent DM-nucleon scattering cross section only at loop level [56,57]); it can also fit the observed gamma-ray galactic center excess [25,58]; and it is a leading benchmark scenario for the DM interpretation of LHC searches [59]). The potential of the 2HDM + a is [34]

$$V = V_{\rm 2HDM} + \frac{\mu_{a_0}^2}{2}a_0^2 + m_\chi\bar{\chi}\chi + \frac{\lambda_a}{4}a_0^4 + \lambda_{a1}a_0^2|H_1|^2 + \lambda_{a2}a_0^2|H_2|^2 + i\kappa a_0 H_1^\dagger H_2 + y_\chi a_0\bar{\chi}i\gamma^5\chi + \mathrm{H.c.} \quad (1)$$

with real pseudoscalar mediator a_0 and Dirac fermion DM χ with mass m_χ, both singlets under the SM gauge interactions. $V_{\rm 2HDM}$ is the 2HDM scalar potential (with a $\mathbb{Z}_2$-symmetry softly broken by a $\mu_{12}^2 H_1^\dagger H_2 + \mathrm{H.c.}$ term in $V_{\rm 2HDM}$, see e.g., [60]). The κ term in (1) yields a mixing θ between a_0 and the 2HDM neutral pseudoscalar state A_0, resulting in two mass eigenstates a, A (with $m_a < m_A$) which provide the portal between the SM and DM.

For a light pseudoscalar a (singlet-like), the coupling between a, h, and Z leads to semidark Higgs decays [a decays to DM particles with a branching fraction $\mathrm{BR}(a \to \chi\bar{\chi}) \simeq 1$ unless $y_\chi \ll 1$]. The partial decay width is $\Gamma(h \to Za) = (m_h^3/16\pi v^2)c_{\beta-\alpha}^2 \sin^2\theta\lambda^{3/2}$, with v the electroweak vacuum expectation value (VEV) and $c_{\beta-\alpha} \equiv \cos(\beta-\alpha)$ parametrizing the deviation from the 2HDM alignment limit [60] (with $\tan\beta = v_2/v_1$, VEV ratio of 2HDM Higgs doublets, and α the mixing angle between the 2HDM CP-even weak eigenstates [61,62]). The model also features an $h \to aa$ decay, leading to a Higgs invisible partial width via $a \to \chi\bar{\chi}$ decays. For $|c_{\beta-\alpha}| \ll 1$, as needed to satisfy the present LHC Higgs signal-strength measurements [63,64], we generally expect $\Gamma(h \to aa) \gg \Gamma(h \to Za)$, yet in certain (albeit small) regions of the 2HDM + a parameter space, the $h \to Za$ semidark Higgs decay can provide stronger sensitivity than the $h \to aa$ invisible Higgs decay, in particular when the $h - a - a$ coupling (see Appendix B for details) vanishes. We consider here a Type-I 2HDM (see [62]) with $c_{\beta-\alpha} = 0.2$, $t_\beta \equiv \tan\beta = 6$, $M = 600$ GeV, $m_{H_0} = m_{H^\pm} = m_{A_0} = 700$ GeV (with $M^2 = \mu_{12}^2/s_\beta c_\beta$ and with $H^\pm$ and H_0 the charged and neutral CP-even heavy 2HDM scalars). We choose in addition $m_\chi = 0.45 m_a$ and y_χ fixed to yield the observed DM relic density via thermal freeze-out (see e.g., [33,58] and Appendix B). We further consider $\lambda_{a1} = \lambda_{a2}$ fixed in each case to the value that yields $\Gamma(h \to aa) = 0$, and show in Fig. 5 the projected LHC sensitivity (with 300 fb^{-1} and at HL-LHC with 3 ab^{-1}) of the semidark Higgs

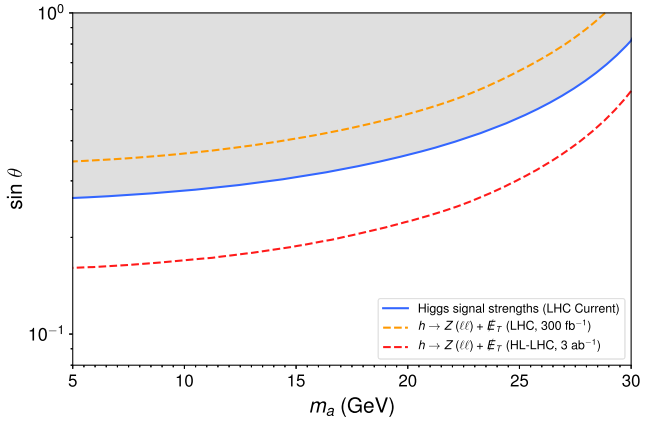

FIG. 5. Present (solid, gray) and projected (dashed) constraints on the $(m_a, \sin\theta)$ plane for the 2HDM + a scenario analyzed in this work (with $\Gamma(h \to aa) = 0$), see text for details.

decay $h \to Z(\ell\ell) + \not{E}_T$ in the $(m_a, \sin\theta)$ parameter space of the 2HDM + a. In addition, while our 2HDM $(c_{\beta-\alpha}, t_\beta)$ benchmark satisfies both present and HL-LHC projected limits from Higgs signal strengths on 2HDM parameters [65], we find using the SCANNERS [66] and HIGGSSIGNALS [67,68] numerical codes that $h \to Za$ exotic Higgs decays in this scenario are currently constrained at 95% confidence level (CL) to $\mathrm{BR}(h \to Za) < 0.042$ from Higgs signal strength measurements. This limit is also shown in Fig. 5. Further details on these constraints, as well as a discussion on other searches that could be sensitive to the 2HDM + a parameter space (yet not to the specific benchmark we choose here) are given in Appendix B.

C. A comment on dark photons

Light dark photons Z_D [69] which interact with the SM via kinetic mixing (see e.g., [70]) give rise to an exotic Higgs decay $h \to ZZ_D$. Invisible dark photons would then constitute another new physics scenario that semidark Higgs decays could be sensitive to. However, current 95% CL bounds on the kinetic mixing parameter ϵ from EW precision observables set $\epsilon < 0.03$ for dark photon masses <30 GeV [71]. The corresponding $h \to ZZ_D$ branching fraction is then $<10^{-3}$ (see e.g., [1]), below the Higgs neutrino floor.

ACKNOWLEDGMENTS

J. M. N. thanks Thomas Biekotter and Olalla Olea for assistance with the use of SCANNERS and HIGGSSIGNALS. J. A. A.-S. acknowledges partial financial support by the Spanish "Agencia Estatal de Investigación" (AEI, MCIN/AEI/10.13039/501100011033) through the Project No. PID2019–110058 GB-C21. The work of J. M. C. was supported by the Spanish MICIU and the EU Fondo Social Europeo (FSE) through the Grant No. PRE2018-083563. The work of J. M. N. was supported by the Ramón y Cajal Fellowship Contract No. RYC-2017-22986, and by Grant No. PGC2018-096646-A-I00 from the Spanish Proyectos de I + D de Generación de Conocimiento. J. M. N. also acknowledges support from the European Union's Horizon 2020 research and innovation programme under the Marie Sklodowska-Curie Grant Agreement No. 860881 (ITN HIDDeN), as well as from the AEI through the IFT Centro de Excelencia Severo Ochoa Grant No. CEX2020-001007-S.

APPENDIX A: DETAILS ON ALP CONSTRAINTS

We here discuss the constraints on the (m_a, f_a) parameter space of an invisibly decaying ALP under the assumptions made in the main text. From [51], we obtain the 95% CL LEP limits from monophoton searches [72,73], which constrain an ALP produced via its coupling to photons and decaying invisibly, as well as the 90% CL limits from $e^+e^- \to \gamma + \not{E}$ (with $\not{E}$ the missing energy of the event) and rare upsilon decays into $\gamma + \not{E}$ from *BABAR* [74,75] (see also [76]) and the projected 90% CL sensitivity of Belle-II in the $\gamma + \not{E}$ final state. Also shown in Fig. 4 are the current 95% CL limits from heavy-ion (Pb-Pb) collisions at the LHC, from ALP searches in light-by-light scattering (as proposed in [77]) performed by ATLAS [78] and CMS [79] (see also [80]). We also include a projection drawn from rescaling the current ATLAS expected sensitivity to an (optimistic) integrated luminosity of 30 nb^{-1}. Finally, we show the bound from the energy loss of supernova 1987A from ALP emission, as taken from [51]. The supernova 1987A limit is stronger than usually quoted for an ALP coupling only to photons since the invisible decay of the ALP allows its corresponding energy to escape the supernova core even for parameter regions with a sizable coupling to photons (contrary to the usual case, where a large enough coupling to photons will result in the ALP being trapped in the core [81]).

We note that the existence of the invisible decay mode of the ALP leads (under the assumptions discussed in the main text) to a strongly suppressed ALP branching fraction to two photons, $\mathrm{BR}(a \to \gamma\gamma) \sim 3 \times 10^{-4}$. Limits from ALP searches in visible final states, like triphoton searches at LEP 1 and LEP 2 via the process $e^+e^- \to \gamma^* \to \gamma a$, $a \to \gamma\gamma$ (as studied in [82,83]), and searches for $Z \to \gamma\gamma$ decays[3] at LEP 1 have to be rescaled by $\mathrm{BR}(a \to \gamma\gamma)$ (assumed to be 100% in [82,83]), and are too weak to appear in Fig. 4. Similarly, the dominant invisible decay of the ALP significantly weakens the limits from beam-dump experiments as compared to the case of visible ALP scenarios

[3]For light ALPs, with masses $\lesssim$10 GeV, the two photons from the ALP decay would appear merged in the detector, and $e^+e^- \to \gamma\gamma$ searches would be sensitive to the presence of the ALP [83].

(see e.g., [84]) roughly by a factor $\mathrm{BR}(a \to \gamma\gamma) \sim 10^{-4}$. A naive rescaling of beam-dump limits results in no meaningful constraints (beyond what is currently excluded by other experiments/observations) from these, and we choose not to include them in Fig. 4. A precise rederivation of these limits requires to additionally take into account the geometry of each experiment to obtain the expected number of $a \to \gamma\gamma$ events in the detector decay volume, which is beyond the scope of this paper.

For an ALP coupled to the hypercharge field strength via $c_{aBB}/f_a a B^{\mu\nu}\tilde{B}_{\mu\nu}$, this introduces a coupling of the ALP to ZZ and $Z\gamma$ (besides the already considered coupling to photons), given respectively by $c_{aZZ}/f_a a Z^{\mu\nu}\tilde{Z}_{\mu\nu}$ and $c_{aZ\gamma}/f_a a F^{\mu\nu}\tilde{Z}_{\mu\nu}$, with $c_{aZZ} = \sin^2\theta_W c_{aBB}$ and $c_{aZ\gamma} = -2\sin\theta_W \cos\theta_W c_{aBB}$ (with θ_W the weak mixing angle). Fixing $c_{aBB} = \alpha_{\mathrm{EM}}/\cos^2\theta_W$ to match the ALP coupling to photons $c_{a\gamma\gamma}$ we assume in the main text, the above limits do not change, yet from $c_{aZ\gamma} \neq 0$ there is another constraint from LEP searches for rare $Z \to \gamma + a$ decays, with a invisible. The L3 collaboration at LEP has set a limit $\mathrm{BR}(Z \to \gamma + a) < 1.1 \times 10^{-6}$ at 90% CL [85], shown in Fig. 6 (in purple) together with the already considered constraints on our scenario (Fig. 4). Other potential bounds from rare Z decays at LEP and LHC, e.g., from $Z \to 3\gamma$ or $Z \to \gamma\ell\ell$ (see [50]), do not lead to meaningful constraints in Fig. 6.

Finally, we comment on the possibility of probing the ALP a via exotic Higgs decays $h \to Za$ with $a \to \gamma\gamma$, as discussed in [50]. We note that, while the corresponding final state allows to consider Higgs production in gluon-fusion (resulting in an $\mathcal{O}(50)$ enhancement of the Higgs production cross section with respect to our scenario, which must rely on Higgs associated production), this is counteracted by the large suppression from $\mathrm{BR}(a \to \gamma\gamma)$. A preliminary study of the LHC sensitivity to ALPs in exotic Higgs decays via $pp \to h \to Za$, $Z \to \ell\ell$, $a \to \gamma\gamma$ including the leading SM backgrounds has been performed in [86], indicating that such decay channel is much less sensitive than the one discussed in this work (given our assumptions for the ALP branching fractions).

APPENDIX B: DETAILS ON 2HDM + a CONSTRAINTS

The main direct experimental probes of the existence of a light ($m_a < 30$ GeV) singletlike pseudoscalar a in the 2HDM + a are the exotic Higgs decays $h \to Za$ (which this work explores in detail) and $h \to aa$. For the latter, the partial width is $\Gamma(h \to aa) = (v^2/32\pi m_h) \times g_{haa}^2 \sqrt{1 - 4m_a^2/m_h^2}$, with the $h - a - a$ coupling g_{haa} given in Eq. (B1). In the main text we have analyzed the tuned scenario $g_{haa} = 0$ (with varying $\lambda_{a1} = \lambda_{a2}$). We now consider the same 2HDM parameter benchmark as in the main text ($c_{\beta-\alpha} = 0.2$, $t_\beta = 6$, $M = 600$ GeV, $m_{H_0} = m_{H^\pm} = m_{A_0} = 700$ GeV), but fix $\lambda_{a1} = \lambda_{a2} = 0$ such that $\Gamma(h \to aa) \neq 0$. The resulting modified LHC sensitivity to the (m_a, $\sin\theta$) parameter space of the 2HDM + a from semidark Higgs decay $h \to Z(\ell\ell) + \not{E}_T$ is shown in Fig. 7. We also depict in Fig. 7 the constraint on the Higgs invisible width from $h \to aa$ decays, which at present is $\mathrm{BR}(h \to \not{E}_T) < 0.11$ at 95% CL [87] under the assumption of SM Higgs production, and is expected to be $\mathrm{BR}(h \to \not{E}_T) < 0.04$ at 95% CL [88] at the HL-LHC.

In addition, LHC Higgs signal strengths constrain the 2HDM + a parameter space for $c_{\beta-\alpha} \neq 0$ and/or $\Gamma(h \to Za)$, $\Gamma(h \to aa) \neq 0$. For $c_{\beta-\alpha} = 0.2$, $t_\beta = 6$, we have performed a global χ^2 fit to present Higgs signal strength measurements via the HIGGSSIGNALS [67,68] numerical code interfaced to SCANNERS [66], yielding the

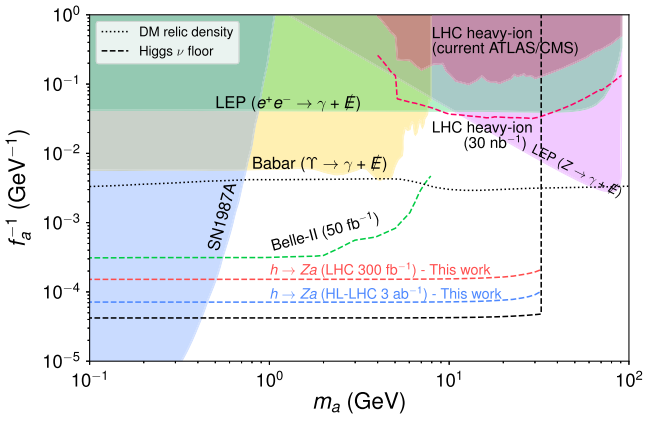

FIG. 6. Present (solid) and projected (dashed) constraints on the (m_a, f_a) plane for an ALP with coupling to the hypercharge field strength, a hidden (DM) fermion χ and the SM Higgs (via a c_{aZh} coupling), see text for details.

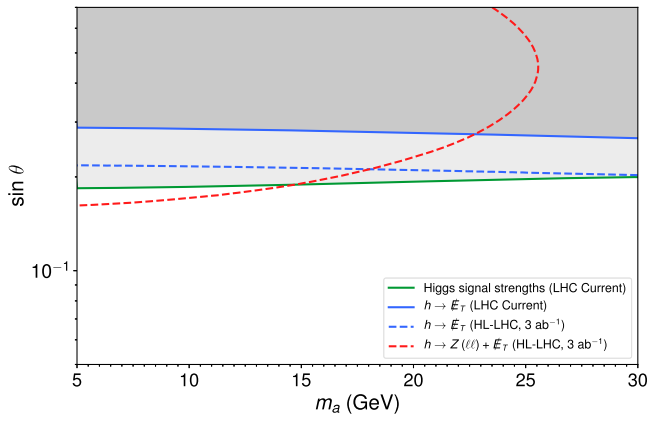

FIG. 7. Present (solid, gray) and projected (dashed) constraints on the (m_a, $\sin\theta$) plane for the 2HDM + a benchmark scenario analyzed in Appendix B [with $\Gamma(h \to aa) \neq 0$], see text for details.

constraint $\mathrm{BR}(h \to Za) + \mathrm{BR}(h \to aa) < 0.042$ at 95% CL, shown in Fig. 7. While this bound will certainly improve at the HL-LHC, the corresponding sensitivity improvement in $\sin\theta$ will only be mild since $\Gamma(h \to Za) \propto \sin^2\theta$ and $\Gamma(h \to aa) \propto \sin^4\theta$ (for our $\lambda_{a1} = \lambda_{a2} = 0$ benchmark), and we expect direct searches for a in exotic Higgs decays to remain competitive with indirect probes through Higgs signal strength measurements.

$$g_{haa} = \left[\frac{2m_a^2}{v^2}s_{\beta-\alpha} + \frac{2(m_{H_0}^2 - M^2) - m_h^2 + (m_{H_0}^2 - m_h^2)[1 + s_{\beta-\alpha}(s_{\beta-\alpha} - c_{\beta-\alpha}(t_\beta - t_\beta^{-1}))]}{v^2}s_{\beta-\alpha} - \lambda_7 c_{\beta-\alpha}\right]s_\theta^2$$
$$+ 2\left(\frac{\lambda_{a1} + t_\beta^2\lambda_{a2}}{1+t_\beta^2}s_{\beta-\alpha} - \frac{(\lambda_{a2} - \lambda_{a1})t_\beta}{1+t_\beta^2}c_{\beta-\alpha}\right)c_\theta^2,$$
$$\lambda_7 = \frac{(M^2 - m_{H_0}^2)(t_\beta - t_\beta^{-1}) - c_{\beta-\alpha}(m_{H_0}^2 - m_h^2)(s_{\beta-\alpha} - c_{\beta-\alpha}(t_\beta - t_\beta^{-1}))}{v^2}. \tag{B1}$$

Other searches for the state a do not provide meaningful sensitivity in the scenario we consider: searches for $h \to aa$ in visible final states (see [14] for a review) like $b\bar{b}\tau\tau$ [10] and $\tau\tau\tau\tau$ [6] are found to be $\mathcal{O}(10^3)$ less sensitive than probes of the Higgs invisible width, and fall short of providing any limit on $\mathrm{BR}(h \to aa)$ by a factor ~50–100, with searches in other final states (e.g., $b\bar{b}\mu\mu$ [8], $\tau\tau\mu\mu$ [4,5]) yielding even smaller sensitivity. Such visible decays of a are then generally not relevant in the 2HDM + a with $m_a > 2m_\chi$, since matching the observed DM relic density requires $y_\chi \sim 1$ (see below), leading to $\mathrm{BR}(a \to \chi\bar{\chi}) > 0.99$ in general. We also find that current LHC mono-jet searches [89] fall short of probing any region of the $(m_a, \sin\theta)$ plane of Figs. 5 and 7 by a factor $\sim 1/(3t_\beta^2)$. Finally, we note that, while the $a - h - Z$ coupling could be constrained via Higgs boson production in association with missing energy at LEP2 through the process $e^+e^- \to Z^* \to ah$, this does not yield meaningful limits on the 2HDM + a parameter space: the searches for $h + \bar{\nu}\nu$ signatures by the OPAL [90], L3 [91], and ALEPH [92,93] experiments at LEP impose a constraint on the missing mass M_{miss} of the event (equal to m_a in our scenario) which is not fulfilled by our signal (e.g., the OPAL analysis [90] requires $50\ \mathrm{GeV} < M_{\mathrm{miss}} < 130\ \mathrm{GeV}$, and it is thus not sensitive to $m_a < 30$ GeV). The corresponding search by the DELPHI experiment [94], while not imposing such a cut on M_{miss}, does not consider Higgs boson masses above 120 GeV.

We also consider possible constraints on the spin-0 states from the 2HDM, $H^\pm$, H_0 and A (doublet-like). Electroweak precision observables (EWPO) constrain (dominantly via the oblique T-parameter) the mass splittings among the 2HDM scalars, since the 2HDM scalar potential of the 2HDM is custodially invariant for $m_{A_0} = m_{H^\pm}$ or $m_{H_0} = m_{H^\pm}$. The latter is chosen for our benchmark scenario, directly satisfying EWPO. Potential constraints from flavor physics, in particular from B-meson decays: $\bar{B} \to X_s\gamma$ decays (which constrain $m_{H^\pm}$ [95,96]) and from $B_s \to \mu^+\mu^-$ (which constrain the presence of a light a coupling to SM fermions [97,98]), are also directly satisfied for a Type-I 2HDM with moderately high t_β (we have chosen in particular $t_\beta = 6$ in our benchmark analysis). Finally, we also discuss direct searches for the 2HDM states as a probe of our scenario; away from the 2HDM alignment limit, $H_0 \to W^+W^-$ and $H_0 \to ZZ$ decays could yield sensitivity if the mass scale of the 2HDM scalars is not very high. At the same time, $H_0 \to Za$ decays would lead to resonant mono-Z signatures [32,34], which have been recently been searched for by the ATLAS experiment [99] (ATLAS also searches for this final state in $H_0 \to ZZ \to \ell\ell\nu\bar{\nu}$ decays [100]). However, in all these cases, we find that for $|s_{\beta-\alpha}t_\beta^{-1} - c_{\beta-\alpha}| \ll 1$ (as our scenario features) the production of H_0 at the LHC is suppressed, and no meaningful limit is obtained.

To conclude, we discuss the need to reproduce the observed DM relic density $\Omega_{\mathrm{DM}}h^2 = 0.12$ [54] within the 2HDM + a, via DM thermal freeze-out in the early Universe. For $m_\chi \gtrsim 2$ GeV, the DM annihilation cross section into SM particles (via $\chi\bar{\chi} \to q_{\mathrm{SM}}q_{\mathrm{SM}}$, with q_{SM} here being generic SM particles) in the nonrelativistic limit is

$$\langle\sigma\mathrm{v}\rangle = \frac{y_\chi^2}{2\pi}\frac{m_\chi^2}{m_a^4 t_\beta^2}s_\theta^2 c_\theta^2\left[\left(1 - \frac{4m_\chi^2}{m_a^2}\right)^2 + \frac{\Gamma_a^2}{m_a^2}\right]^{-1}$$
$$\times \sum_f N_C \frac{m_f^2}{v^2}\sqrt{1 - \frac{m_f^2}{m_a^2}}. \tag{B2}$$

with Γ_a the decay width of a. The sum over SM fermion f annihilation channels involves quarks ($N_C = 3$) and charged leptons ($N_C = 1$). Reproducing the observed DM relic density via thermal freeze-out requires $\langle\sigma\mathrm{v}\rangle \simeq 3 \times 10^{-26}\ \mathrm{cm}^3/\mathrm{s}$, which generically leads to $\mathcal{O}(1)$ values for y_χ. For $m_\chi < 2$ GeV the DM annihilation into SM fermions (b, c-quarks and/or τ-leptons, depending on m_χ) ceases to be the dominant DM annihilation process, and instead annihilation into QCD hadrons (via the 1-loop coupling of a to gluons) dominates. Due to its complexity, we do not study that region of the 2HDM + a parameter space, which may also involve $y_\chi \gg 1$, in this work.

[1] D. Curtin *et al.*, Exotic decays of the 125 GeV Higgs boson, Phys. Rev. D **90**, 075004 (2014).

[2] A. Tumasyan *et al.* (CMS Collaboration), Search for low-mass dilepton resonances in Higgs boson decays to four-lepton final states in proton–proton collisions at $\sqrt{s} = 13$ TeV, Eur. Phys. J. C **82**, 290 (2022).

[3] G. Aad *et al.* (ATLAS Collaboration), Search for Higgs bosons decaying into new spin-0 or spin-1 particles in four-lepton final states with the ATLAS detector with 139 fb^{-1} of pp collision data at $\sqrt{s} = 13$ TeV, J. High Energy Phys. 03 (2022) 041.

[4] A. M. Sirunyan *et al.* (CMS Collaboration), Search for a light pseudoscalar Higgs boson in the boosted $\mu\mu\tau\tau$ final state in proton-proton collisions at $\sqrt{s} = 13$ TeV, J. High Energy Phys. 08 (2020) 139.

[5] A. M. Sirunyan *et al.* (CMS Collaboration), Search for an exotic decay of the Higgs boson to a pair of light pseudoscalars in the final state of two muons and two τ leptons in proton-proton collisions at $\sqrt{s} = 13$ TeV, J. High Energy Phys. 11 (**2018**) 018.

[6] A. M. Sirunyan *et al.* (CMS Collaboration), Search for light pseudoscalar boson pairs produced from decays of the 125 GeV Higgs boson in final states with two muons and two nearby tracks in pp collisions at $\sqrt{s} = 13$ TeV, Phys. Lett. B **800**, 135087 (2020).

[7] G. Aad *et al.* (ATLAS Collaboration), Search for Higgs boson decays into two new low-mass spin-0 particles in the $4b$ channel with the ATLAS detector using pp collisions at $\sqrt{s} = 13$ TeV, Phys. Rev. D **102**, 112006 (2020).

[8] G. Aad *et al.* (ATLAS Collaboration), Search for Higgs boson decays into a pair of pseudoscalar particles in the $bb\mu\mu$ final state with the ATLAS detector in pp collisions at $\sqrt{s} = 13$ TeV, Phys. Rev. D **105**, 012006 (2022).

[9] A. M. Sirunyan *et al.* (CMS Collaboration), Search for an exotic decay of the Higgs boson to a pair of light pseudoscalars in the final state with two muons and two b quarks in pp collisions at 13 TeV, Phys. Lett. B **795**, 398 (2019).

[10] A. M. Sirunyan *et al.* (CMS Collaboration), Search for an exotic decay of the Higgs boson to a pair of light pseudoscalars in the final state with two b quarks and two τ leptons in proton-proton collisions at $\sqrt{s} = 13$ TeV, Phys. Lett. B **785**, 462 (2018).

[11] M. Aaboud *et al.* (ATLAS Collaboration), Search for the Higgs boson produced in association with a vector boson and decaying into two spin-zero particles in the $H \to aa \to 4b$ channel in pp collisions at $\sqrt{s} = 13$ TeV with the ATLAS detector, J. High Energy Phys. 10 (2018) 031.

[12] M. Aaboud *et al.* (ATLAS Collaboration), Search for Higgs boson decays into pairs of light (pseudo)scalar particles in the $\gamma\gamma jj$ final state in pp collisions at $\sqrt{s} =$ 13 TeV with the ATLAS detector, Phys. Lett. B **782**, 750 (2018).

[13] G. Aad *et al.* (ATLAS Collaboration), Search for Higgs Boson Decays into a Z Boson and a Light Hadronically Decaying Resonance Using 13 TeV pp Collision Data from the ATLAS Detector, Phys. Rev. Lett. **125**, 221802 (2020).

[14] M. Cepeda, S. Gori, V. M. Outschoorn, and J. Shelton, Exotic Higgs decays, arXiv:2111.12751.

[15] C. Englert, M. Spannowsky, and C. Wymant, Partially (in)visible Higgs decays at the LHC, Phys. Lett. B **718**, 538 (2012).

[16] C. Petersson, A. Romagnoni, and R. Torre, Higgs decay with monophoton + MET signature from low scale supersymmetry breaking, J. High Energy Phys. 10 (2012) 016.

[17] V. Khachatryan *et al.* (CMS Collaboration), Search for exotic decays of a Higgs boson into undetectable particles and one or more photons, Phys. Lett. B **753**, 363 (2016).

[18] A. M. Sirunyan *et al.* (CMS Collaboration), Search for dark photons in decays of Higgs bosons produced in association with Z bosons in proton-proton collisions at $\sqrt{s} = 13$ TeV, J. High Energy Phys. 10 (2019) 139.

[19] A. M. Sirunyan *et al.* (CMS Collaboration), Search for dark photons in Higgs boson production via vector boson fusion in proton-proton collisions at $\sqrt{s} = 13$ TeV, J. High Energy Phys. 03 (2021) 011.

[20] G. Aad *et al.* (ATLAS Collaboration), Observation of electroweak production of two jets in association with an isolated photon and missing transverse momentum, and search for a Higgs boson decaying into invisible particles at 13 TeV with the ATLAS detector, Eur. Phys. J. C **82**, 105 (2022).

[21] G. Aad *et al.* (ATLAS Collaboration), Search for exotic decays of the Higgs boson into $b\bar{b}$ and missing transverse momentum in pp collisions at $\sqrt{s} = 13$ TeV with the ATLAS detector, J. High Energy Phys. 01 (2022) 063.

[22] E. Aprile *et al.* (XENON Collaboration), Dark Matter Search Results from a One Ton-Year Exposure of XENON1T, Phys. Rev. Lett. **121**, 111302 (2018).

[23] C. Boehm, M. J. Dolan, C. McCabe, M. Spannowsky, and C. J. Wallace, Extended gamma-ray emission from coy dark matter, J. Cosmol. Astropart. Phys. 05 (2014) 009.

[24] E. Izaguirre, G. Krnjaic, and B. Shuve, The galactic center excess from the bottom up, Phys. Rev. D **90**, 055002 (2014).

[25] S. Ipek, D. McKeen, and A. E. Nelson, A renormalizable model for the galactic center gamma ray excess from dark matter annihilation, Phys. Rev. D **90**, 055021 (2014).

[26] L. Goodenough and D. Hooper, Possible evidence for dark matter annihilation in the inner Milky Way from the fermi gamma ray space telescope, arXiv:0910.2998.

[27] D. Hooper and L. Goodenough, Dark matter annihilation in the galactic center as seen by the fermi gamma ray space telescope, Phys. Lett. B **697**, 412 (2011).

[28] M. Ajello *et al.* (Fermi-LAT Collaboration), Fermi-LAT observations of high-energy γ-ray emission toward the galactic center, Astrophys. J. **819**, 44 (2016).

[29] J. Monroe and P. Fisher, Neutrino backgrounds to dark matter searches, Phys. Rev. D **76**, 033007 (2007).

[30] D. de Florian *et al.* (LHC Higgs Cross Section Working Group Collaboration), Handbook of LHC Higgs cross sections: 4. Deciphering the nature of the Higgs sector, arXiv:1610.07922.

[31] A. Alloul, N. D. Christensen, C. Degrande, C. Duhr, and B. Fuks, FeynRules 2.0—A complete toolbox for tree-level phenomenology, Comput. Phys. Commun. **185**, 2250 (2014).

[32] J. M. No, Looking through the pseudoscalar portal into dark matter: Novel mono-Higgs and mono-Z signatures at the LHC, Phys. Rev. D **93**, 031701 (2016).
[33] D. Goncalves, P. A. N. Machado, and J. M. No, Simplified models for dark matter face their consistent completions, Phys. Rev. D **95**, 055027 (2017).
[34] M. Bauer, U. Haisch, and F. Kahlhoefer, Simplified dark matter models with two Higgs doublets: I. Pseudoscalar mediators, J. High Energy Phys. 05 (2017) 138.
[35] J. Alwall, R. Frederix, S. Frixione, V. Hirschi, F. Maltoni, O. Mattelaer, H.-S. Shao, T. Stelzer, P. Torrielli, and M. Zaro, The automated computation of tree-level and next-to-leading order differential cross sections, and their matching to parton shower simulations, J. High Energy Phys. 07 (2014) 079.
[36] V. Bertone, S. Carrazza, N. P. Hartland, and J. Rojo (NNPDF Collaboration), Illuminating the photon content of the proton within a global PDF analysis, SciPost Phys. **5**, 008 (2018).
[37] T. Sjöstrand, S. Ask, J. R. Christiansen, R. Corke, N. Desai, P. Ilten, S. Mrenna, S. Prestel, C. O. Rasmussen, and P. Z. Skands, An introduction to PYTHIA 8.2, Comput. Phys. Commun. **191**, 159 (2015).
[38] J. de Favereau, C. Delaere, P. Demin, A. Giammanco, V. Lemaître, A. Mertens, and M. Selvaggi (DELPHES 3 Collaboration), DELPHES 3, A modular framework for fast simulation of a generic collider experiment, J. High Energy Phys. 02 (2014) 057.
[39] T. Binoth, G. Ossola, C. Papadopoulos, and R. Pittau, NLO QCD corrections to tri-boson production, J. High Energy Phys. 06 (2008) 082.
[40] A. Kulesza, L. Motyka, D. Schwartländer, T. Stebel, and V. Theeuwes, Associated production of a top quark pair with a heavy electroweak gauge boson at nlo + nnll accuracy, Eur. Phys. J. C **79**, 249 (2019).
[41] F. Cascioli, T. Gehrmann, M. Grazzini, S. Kallweit, P. Maierhöfer, A. von Manteuffel, S. Pozzorini, D. Rathlev, L. Tancredi, and E. Weihs, Zz production at hadron colliders in nnlo QCD, Phys. Lett. B **735**, 311 (2014).
[42] S. Frixione, E. Laenen, P. Motylinski, B. R. Webber, and C. D. White, Single-top hadroproduction in association with a W boson, J. High Energy Phys. 07 (2008) 029.
[43] H. E. Faham, F. Maltoni, K. Mimasu, and M. Zaro, Single top production in association with a WZ pair at the LHC in the SMEFT, J. High Energy Phys. 01 (2022) 100.
[44] ATLAS Collaboration, Trigger menu in 2018, Report No. ATL-DAQ-PUB-2019-001, CERN, 2019.
[45] G. Cowan, K. Cranmer, E. Gross, and O. Vitells, Asymptotic formulae for likelihood-based tests of new physics, Eur. Phys. J. C **71**, 1554 (2011).
[46] T. Behnke *et al.*, The international linear collider technical design report—Volume 1: Executive summary, arXiv:1306.6327.
[47] P. Bambade, T. Barklow, T. Behnke, M. Berggren, J. Brau, P. Burrows *et al.*, The international linear collider: A global project, arXiv:1903.01629.
[48] C. T. Potter, DSiD: A delphes detector for ILC physics studies, in *International Workshop on Future Linear Colliders* (2016), arXiv:1602.07748.
[49] I. Brivio, M. B. Gavela, L. Merlo, K. Mimasu, J. M. No, R. del Rey, and V. Sanz, ALPs effective field theory and collider signatures, Eur. Phys. J. C **77**, 572 (2017).
[50] M. Bauer, M. Neubert, and A. Thamm, Collider probes of axion-like particles, J. High Energy Phys. 12 (2017) 044.
[51] M. J. Dolan, T. Ferber, C. Hearty, F. Kahlhoefer, and K. Schmidt-Hoberg, Revised constraints and Belle II sensitivity for visible and invisible axion-like particles, J. High Energy Phys. 12 (2017) 094.
[52] A. Alves, A. G. Dias, and D. D. Lopes, Probing ALP-sterile neutrino couplings at the LHC, J. High Energy Phys. 08 (2020) 074.
[53] G. Alonso-Álvarez, M. B. Gavela, and P. Quilez, Axion couplings to electroweak gauge bosons, Eur. Phys. J. C **79**, 223 (2019).
[54] P. A. R. Ade *et al.* (Planck Collaboration), Planck 2015 results. XIII. Cosmological parameters, Astron. Astrophys. **594**, A13 (2016).
[55] T. Robens, The THDMa revisited, Symmetry **13**, 2341 (2021).
[56] F. Ertas and F. Kahlhoefer, Loop-induced direct detection signatures from *CP*-violating scalar mediators, J. High Energy Phys. 06 (2019) 052.
[57] T. Abe, M. Fujiwara, J. Hisano, and Y. Shoji, Maximum value of the spin-independent cross section in the 2HDM + a, J. High Energy Phys. 01 (2020) 114.
[58] P. Tunney, J. M. No, and M. Fairbairn, Probing the pseudoscalar portal to dark matter via $\bar{b}bZ(\to\ell\ell)+\not{E}_T$: From the LHC to the galactic center excess, Phys. Rev. D **96**, 095020 (2017).
[59] T. Abe *et al.* (LHC Dark Matter Working Group), LHC Dark Matter Working Group: Next-generation spin-0 dark matter models, Phys. Dark Universe **27**, 100351 (2020).
[60] J. F. Gunion and H. E. Haber, The *CP* conserving two Higgs doublet model: The approach to the decoupling limit, Phys. Rev. D **67**, 075019 (2003).
[61] J. F. Gunion, H. E. Haber, G. L. Kane, and S. Dawson, *The Higgs Hunter's Guide* (CRC Press, United States, 2000), Vol. 80.
[62] G. Branco, P. Ferreira, L. Lavoura, M. Rebelo, M. Sher, and J. P. Silva, Theory and phenomenology of two-Higgs-doublet models, Phys. Rep. **516**, 1 (2012).
[63] CMS Collaboration, Combined Higgs boson production and decay measurements with up to 137 fb^{-1} of proton-proton collision data at $\sqrt{s}=13$ TeV, Report No. CMS-PAS-HIG-19-005 CERN, 2020.
[64] ATLAS Collaboration, A combination of measurements of Higgs boson production and decay using up to 139 fb^{-1} of proton–proton collision data at $\sqrt{s}=13$ TeV collected with the ATLAS experiment, Report No. ATLAS-CONF-2020-027, CERN, 2020.
[65] ATLAS Collaboration, Prospects for new physics in Higgs couplings studies with the ATLAS detector at the HL-LHC, Report No. ATL-PHYS-PUB-2014-017, CERN, 2014.
[66] M. Mühlleitner, M. O. P. Sampaio, R. Santos, and J. Wittbrodt, ScannerS: Parameter scans in extended scalar sectors, Eur. Phys. J. C **82**, 198 (2022).
[67] P. Bechtle, S. Heinemeyer, O. Stål, T. Stefaniak, and G. Weiglein, HiggsSignals: Confronting arbitrary Higgs

sectors with measurements at the Tevatron and the LHC, Eur. Phys. J. C **74**, 2711 (2014).
[68] P. Bechtle, S. Heinemeyer, T. Klingl, T. Stefaniak, G. Weiglein, and J. Wittbrodt, HiggsSignals-2: Probing new physics with precision Higgs measurements in the LHC 13 TeV era, Eur. Phys. J. C **81**, 145 (2021).
[69] M. Fabbrichesi, E. Gabrielli, and G. Lanfranchi, The dark photon, arXiv:2005.01515.
[70] J. Jaeckel, M. Jankowiak, and M. Spannowsky, LHC probes the hidden sector, Phys. Dark Universe **2**, 111 (2013).
[71] A. Hook, E. Izaguirre, and J. G. Wacker, Model independent bounds on kinetic mixing, Adv. High Energy Phys. **2011**, 859762 (2011).
[72] P. J. Fox, R. Harnik, J. Kopp, and Y. Tsai, LEP shines light on dark matter, Phys. Rev. D **84**, 014028 (2011).
[73] J. Abdallah *et al.* (DELPHI Collaboration), Search for one large extra dimension with the DELPHI detector at LEP, Eur. Phys. J. C **60**, 17 (2009).
[74] P. del Amo Sanchez *et al.* (*BABAR* Collaboration), Search for Production of Invisible Final States in Single-Photon Decays of $\Upsilon(1S)$, Phys. Rev. Lett. **107**, 021804 (2011).
[75] B. Aubert *et al.* (*BABAR* Collaboration), Search for invisible decays of a light scalar in radiative transitions $v_{3S} \to \gamma$ A0, in *Proceedings of the 34th International Conference on High Energy Physics* (Princeton University Trustees, United States, 2008), arXiv:0808.0017.
[76] D. Antreasyan *et al.* (Crystal Ball Collaboration), Limits on axion and light Higgs boson production in Upsilon (1s) decays, Phys. Lett. B **251**, 204 (1990).
[77] S. Knapen, T. Lin, H. K. Lou, and T. Melia, Searching for Axionlike Particles with Ultraperipheral Heavy-Ion Collisions, Phys. Rev. Lett. **118**, 171801 (2017).
[78] G. Aad *et al.* (ATLAS Collaboration), Measurement of light-by-light scattering and search for axion-like particles with 2.2 nb^{-1} of Pb + Pb data with the ATLAS detector, J. High Energy Phys. 11 (**2021**) 050.
[79] A. M. Sirunyan *et al.* (CMS Collaboration), Evidence for light-by-light scattering and searches for axion-like particles in ultraperipheral PbPb collisions at $\sqrt{s_{\mathrm{NN}}} = 5.02$ TeV, Phys. Lett. B **797**, 134826 (2019).
[80] J. Bonilla, I. Brivio, J. Machado-Rodríguez, and J. F. de Trocóniz, Nonresonant searches for axion-like particles in vector boson scattering processes at the LHC, J. High Energy Phys. 06 (2022) 113.
[81] G. G. Raffelt, Astrophysical axion bounds, Lect. Notes Phys. **741**, 51 (2008).
[82] K. Mimasu and V. Sanz, ALPs at colliders, J. High Energy Phys. 06 (2015) 173.
[83] J. Jaeckel and M. Spannowsky, Probing MeV to 90 GeV axion-like particles with LEP and LHC, Phys. Lett. B **753**, 482 (2016).
[84] B. Döbrich, J. Jaeckel, F. Kahlhoefer, A. Ringwald, and K. Schmidt-Hoberg, ALPtraum: ALP production in proton beam dump experiments, J. High Energy Phys. 02 (2016) 018.
[85] M. Acciarri *et al.* (L3 Collaboration), Search for new physics in energetic single photon production in e^+e^- annihilation at the Z resonance, Phys. Lett. B **412**, 201 (1997).
[86] G. Brooijmans *et al.*, Les Houches 2019 Physics at TeV colliders: New physics working group report, in *Proceedings of the 11th Les Houches Workshop on Physics at TeV Colliders: PhysTeV Les Houches* (2020), arXiv:2002.12220.
[87] ATLAS Collaboration, Combination of searches for invisible Higgs boson decays with the ATLAS experiment, Report No. ATLAS-CONF-2020-052, CERN, 2020.
[88] CMS Collaboration, Search for invisible decays of a Higgs boson produced through vector boson fusion at the High-Luminosity LHC, Report No. CMS-PAS-FTR-18-016, CERN, 2018.
[89] CMS Collaboration, Search for new particles in events with energetic jets and large missing transverse momentum in proton-proton collisions at $\sqrt{s} = 13$ TeV, Report No. CMS-PAS-EXO-20-004, CERN, 2021.
[90] G. Abbiendi *et al.* (OPAL Collaboration), Search for the standard model Higgs boson with the OPAL detector at LEP, Eur. Phys. J. C **26**, 479 (2003).
[91] P. Achard *et al.* (L3 Collaboration), Standard model Higgs boson with the L3 experiment at LEP, Phys. Lett. B **517**, 319 (2001).
[92] A. Heister *et al.* (ALEPH Collaboration), Final results of the searches for neutral Higgs bosons in e^+ e^- collisions at s up to 209-GeV, Phys. Lett. B **526**, 191 (2002).
[93] R. Barate *et al.* (ALEPH Collaboration), Observation of an excess in the search for the standard model Higgs boson at ALEPH, Phys. Lett. B **495**, 1 (2000).
[94] J. Abdallah *et al.* (DELPHI Collaboration), Final results from DELPHI on the searches for SM and MSSM neutral Higgs bosons, Eur. Phys. J. C **32**, 145 (2004).
[95] T. Hermann, M. Misiak, and M. Steinhauser, $\bar{B} \to X_s\gamma$ in the two Higgs doublet model up to next-to-next-to-leading order in QCD, J. High Energy Phys. 11 (2012) 036.
[96] M. Misiak, A. Rehman, and M. Steinhauser, Towards $\bar{B} \to X_s\gamma$ at the NNLO in QCD without interpolation in m_c, J. High Energy Phys. 06 (**2020**) 175.
[97] W. Skiba and J. Kalinowski, $B_s \to \tau^+\tau^-$ decay in a two Higgs doublet model, Nucl. Phys. **B404**, 3 (1993).
[98] H. E. Logan and U. Nierste, $B_{s,d} \to \ell^+\ell^-$ in a two Higgs doublet model, Nucl. Phys. **B586**, 39 (2000).
[99] G. Aad *et al.* (ATLAS Collaboration), Search for associated production of a Z boson with an invisibly decaying Higgs boson or dark matter candidates at $s = 13$ TeV with the ATLAS detector, Phys. Lett. B **829**, 137066 (2022).
[100] G. Aad *et al.* (ATLAS Collaboration), Search for heavy resonances decaying into a pair of Z bosons in the $\ell^+\ell^-\ell'^+\ell'^-$ and $\ell^+\ell^-\nu\bar{\nu}$ final states using 139 fb^{-1} of proton–proton collisions at $\sqrt{s} = 13$ TeV with the ATLAS detector, Eur. Phys. J. C **81**, 332 (2021).